Anterior scleral thickness in Marfan syndrome: a quantitative analysis

Authors

Lien ALLUYN[1], Laure DEQUEKER[2], Siska DHAESE[3], Alejandra CONSEJO[4], Julie DE ZAEYTIJD[1], Bart P. LEROY[1,5,6], Julie DE BACKER[5,7,8], Elke O. KREPS[1]

1. Department of Ophthalmology, Ghent University Hospital, Ghent, Belgium
2. Department of Ophthalmology, AZ Groeninge, Kortrijk, Belgium
3. Eyeclinic 't Zand Bruges, Bruges, Belgium
4. Aragon Institute for Engineering Research (I3A), University of Zaragoza, Zaragoza, Spain
5. Center for Medical Genetics, Ghent University Hospital, Ghent, Belgium
6. Division of Ophthalmology & Center for Cellular & Molecular Therapeutics, Children's Hospital of Philadelphia, Philadelphia, PA, United States
7. Department of Biomolecular Medicine, Faculty of Medicine and Health Sciences, Ghent University, Ghent, Belgium
8. Department of Cardiology, Ghent University Hospital, Ghent, Belgium

Correspondence:
Elke O. KREPS
Elke.kreps@ugent.be
Department of Ophthalmology
Ghent University Hospital
Corneel Heymanslaan 10
9000 Ghent
Belgium
Tel: +32 93322306
Fax: /

ABSTRACT

Purpose: To investigate the anterior scleral thickness (AST) in patients with Marfan syndrome (MFS).

Methods: A prospective, cross-sectional study was conducted at the Department of Ophthalmology, Ghent University Hospital, Ghent including patients with a genetically confirmed clinical diagnosis of MFS and age-, gender- and axial length-matched controls. Subjects with known corneal, conjunctival or scleral pathology and a history of ocular surgery, including pars plana vitrectomy, recent contact lens use, or high-grade astigmatism were excluded. Subjects underwent non-cycloplegic autorefraction, Scheimpflug-based corneal tomography, axial length measurement and spectral-domain optical coherence tomography (OCT). AST was manually measured at 1mm (AST1), 2mm (AST2) and 3mm (AST3) from the scleral spur temporally and nasally.

Results: A total of 56 subjects (28 subjects in the MFS group and 28 matched in the control group) were included in this study. In patients with MFS, AST was significantly reduced compared to matched controls, both overall and at every analysed measuring point in the nasal and temporal area ($p<0.001$). Central corneal thickness (CCT) and mean keratometry (Kmean) values were significantly lower in patients with MFS ($p<0.05$). A positive correlation was found between nasal AST and CCT in patients with MFS. No correlation was found between AST and Kmean, nor between AST and axial length. In patients with MFS with ectopia lentis compared to those without, temporal AST3 was significantly lower ($p<0.05$). AST was significantly lower in patients with MFS harbouring a variant predicted to cause haploinsufficiency compared to those with a variant expected to lead to a dominant negative effect for both nasal and temporal measurements.

Conclusion: Based on anterior segment OCT measurements, AST of patients with MFS is significantly lower compared to matched controls.

Keywords: Marfan syndrome, anterior scleral thickness, sclera, optical coherence tomography

INTRODUCTION

The sclera plays a vital role in protecting the intraocular structures, blocking off-axis light scatter, and maintaining optical stability under dynamic conditions imposed by intraocular pressure fluctuations and eye movements (Boote et al. 2020). Like other connective tissues, the sclera is primarily a scaffold of fibrous collagen, interspersed with elastic microfibrils, in a hydrated interfibrillar matrix of proteoglycans and glycoproteins. Mature scleral elastic fibres consist of an amorphous elastin core sheathed by an aligned scaffold of fibrillin-rich microfibrils (Boote et al. 2020). Marfan syndrome (MFS) is a multisystem, genetic disorder associated with pathogenic variants in the fibrillin-1 (*FBN1*) gene. Although diagnosis is primarily clinical, based on Ghent II nosology, genetic testing can aid in distinguishing MFS from other connective tissue disorders (Loeys et al. 2010; Milewicz et al. 2021). Disproportionately long extremities, aortic root aneurysms, and ectopia lentis are among the most characteristic features (Milewicz et al. 2021). Due to the widespread distribution of fibrillin-1 containing microfibrils throughout the eye, ocular manifestations in MFS are variable. Many studies have focused on ocular biometry and corneal features in patients with MFS, whereas research into scleral characteristics – in large part due to the inherent difficulties in imaging this opaque and peripheral tissue – is scarce. Case reports of spontaneous and postoperative (early and late onset) scleral perforations in patients with MFS suggest MFS-related changes to the scleral architecture (Rodríguez-Ares et al. 1999; Deramo et al. 2001; Oyewole et al. 2011; Sharifipour et al. 2013; Turaga et al. 2016; Voulgari et al. 2019; Stanciu et al. 2022). Scleral thinning in patients with MFS has also been described based on slit-lamp observations (Sharifipour et al. 2013; Turaga et al. 2016). The increased axial length and higher risk of open-angle glaucoma observed in MFS cohorts may also reflect fibrillin-related changes to the scleral development and function (Nemet et al. 2006; Milewicz et al. 2021). One prior study demonstrated significant changes to the shape of the sclera in patients with MFS (Vanhonsebrouck et al. 2021), yet scleral thickness in patients with MFS has not been studied in further detail. The sclera is, however, a frequently targeted area for surgical interventions in patients with MFS, resulting in a need for further understanding of the scleral characteristics in these patients. The introduction of spectral-domain optical coherence technology (SD-OCT) with anterior segment modules has enabled non-contact, high-resolution imaging of ocular structures including the anterior sclera (Wojtkowski et al. 2004). The aim of this study was to evaluate OCT-based anterior scleral thickness (AST) in patients with MFS as compared to age- and axial length matched controls. As a secondary analysis, correlations between scleral thickness and the clinical and genetic characteristics of MFS were explored.

MATERIALS AND METHODS

A cross-sectional, case-control study was conducted at the Department of Ophthalmology of Ghent University Hospital, Belgium. The study group consisted of patients with MFS and age-, gender- and axial length-matched controls. The diagnosis of MFS was based on clinical features using the Ghent II diagnostic criteria, genetic confirmation through *FBN1* pathogenic variant analysis, or both. Exclusion criteria included the presence of corneal, conjunctival, or scleral pathology, and a history of scleral surgery including pars plana vitrectomy. Subjects with any history of ocular surgery, known corneal diseases (e.g. keratoconus, pellucid marginal degeneration, corneal scars, corneal dystrophy), recent use (<14 days) of rigid gas permeable or soft contact lenses, known connective tissue disorder, and astigmatism greater than 3.5 dioptre were excluded. The study protocol was approved by the institutional Ethics Committee and all participants provided written informed consent before commencement of the study.

The following procedures were performed during a single visit in all patients: non-cycloplegic autorefraction (Nidek Ark-510A, Nidek Co., Ltd, Aichi, Japan), Scheimpflug-based corneal tomography (Pentacam HR; Oculus, Wetzlar, Germany), ocular biometry (IOLMaster 700; Carl Zeiss Meditec AG, Oberkochen, Germany) and SD-OCT (Spectralis Anterior Segment Module, Heidelberg Engineering, Dossenheim, Germany). Perilimbal scleral OCT scans were acquired in sclera mode with the enhanced-depth imaging (EDI) mode active. Volume scans with eleven sections were acquired with the OCT image scan angle set at 15°. The images had a resolution of 768 x 496 pixels. Measurements were taken at 3- and 9-o'clock positions, for which the participants were asked to look at an external fixation point opposite to the examined scleral area. These fixation marks were established on the wall prior to the measurements at an angle of 45° from the central axis of the device. The external fixation allowed image acquisition encompassing the limbus and the sclera up to 3mm posterior to the scleral spur while ensuring stable and consistent fixation. Patients were asked to firmly fixate the chin and forehead to the device to minimize any eye or head position changes during image acquisition. Scleral thickness was measured manually at 1 mm (AST1), 2 mm (AST2) and 3 mm (AST3) from the scleral spur, perpendicularly to the conjunctival surface. The apex of the scleral spur, where the sclera protrudes slightly and the ciliary muscle inserts, served as the reference point for measurements (see Figure 1). To validate the measurement procedure, a repeatability analysis was conducted: three measurements were taken by the same examiner from single right eyes of thirty additional healthy participants, who were not included in the control group of the study. Participants were instructed to reposition before each measurement, allowing a brief break in between measurements. The coefficient of variation (CV) was calculated as an indicator of repeatability. We opted to analyse full-thickness measurements, as applied in the study by Kommula and associates, for the following reasons: discrimination of the different layers (conjunctival/episcleral/sclera) is not commercially available at present, there is uncertainty regarding the correct definitions of the different layers on OCT images and reproducibility analysis of layer discrimination in recent research has demonstrated only moderate reproducibility (Kommula et al. 2023; Teeuw et al. 2023).

Variants of *FBN1* were identified and their level of pathogenicity determined according to the adjusted American College of Medical Genetics and Genomics and the Association for Molecular Pathology (ACMG/AMP) guidelines (Muiño-Mosquera et al. 2018). Subsequently, (likely) pathogenic variants in the *FBN1* gene were categorised into missense, in-frame, nonsense, frameshift, and splice-site variants. Variants were also classified based on their anticipated impact on fibrillin-1. Nonsense and frameshift variants not affecting exon 65 or the last 50 nucleotides of exon 64 were considered to have a haploinsufficient effect (Muiño-Mosquera et al. 2020). Haploinsufficiency results in a decreased quantity of functional protein. The other nonsense and frameshift variants and all missense variants were considered to lead to abnormal or shorter yet stable protein, thus exerting a dominant negative effect. This classification approach aligns with the framework established by Muiño-Mosquera et al. (Muiño-Mosquera et al. 2020). Splice-site variants cause alterations that commonly result in a frame-shift, premature termination codon, and ultimately nonsense mediated decay (Holbrook et al. 2004; Linde & Kerem 2008; Popp & Maquat 2016). Splice-site variants were therefore considered to exert a haploinsufficient effect.

Statistical analysis was performed using SPSS software (version 28, SPSS, Inc). Descriptive data were assessed for normality using the Shapiro-Wilk test, followed by independent Student's t-tests. To compare AST between MFS and control groups, a three-way repeated measures ANOVA was conducted to examine the effects of group (Marfan vs. control), area analysed (nasal vs. temporal), and distance from the scleral spur (1mm, 2mm, and 3mm), as well as their interactions. Assumptions of normality, sphericity (Mauchly's test), and homogeneity of variances (Levene's test) were met. Post-hoc comparisons were performed using the Bonferroni test. For subsequent sections, independent or paired Student's t-tests were used for normally distributed data, while the Mann-Whitney *U* test was used for skewed data. The effect of different *FBN1* (likely) pathogenic variants on AST was analysed using one-way ANOVA and the Bonferroni post-hoc test. A significance level of 0.05 was used.

RESULTS

A total of 56 subjects (28 subjects in the MFS group and 28 matched in the control group) were included in the main analysis. Study group characteristics are shown in Table 1 and clinical and genetic data of the MFS group are listed in Table 2. To eliminate interocular correlations, one eye per patient was included for statistical analysis. In all subjects, right eyes were included, expect for two controls and three Marfan patients, in which the left eye was included. There were no significant differences between patients and controls in age ($p=0.45$), gender ($p>0.999$), axial length ($p=0.94$) or spherical equivalent ($p=0.35$), as determined by independent t-tests. Prior to the study, repeatability of the OCT-measurement protocol was assessed as described above. The CV values were below 1% for all cases, indicating very good repeatability. Specifically, the CV values were 0.92%, 0.74%, and 0.79% for AST1, AST2, and AST3 in the nasal region, and 0.68%, 0.75%, and 0.63% for AST1, AST2, and AST3 in the temporal region for the right eyes.

When assessing the entire group, AST was significantly thinner in the temporal region (670 ± 90 µm) compared to the nasal region (711 ± 85 µm) (three-way ANOVA, $F(1, 167)=23.97$, $p<0.001$, $\eta_p^2=0.07$). With increasing distance to the scleral spur, AST also increased (1mm: 678 ± 86µm, 2mm: 683 ± 87 µm, 3mm: 712 ± 93 µm) (three-way ANOVA, $F(2, 222)=6.15$, $p=0.002$, $\eta_p^2=0.04$). Moreover, the increase in AST with distance was more pronounced in the nasal area compared to the temporal area (three-way ANOVA, $F(2, 222)=4.98$, $p=0.01$, $\eta_p^2=0.03$). The Bonferroni post-hoc test indicated a significant difference in AST between 1mm and 3mm ($p=0.004$), between 2mm and 3mm ($p=0.018$), but no significant difference between 1mm and 2mm ($p>0.999$).

The AST values for the MFS and control groups are presented in Table 3. Overall, eyes with MFS had significantly lower AST values (652 ± 82 µm) compared to control eyes (729 ± 80 µm) (three-way ANOVA, $F (1, 167) = 84.98$, $p<0.001$, $\eta_p^2=0.21$). The difference in AST values was statistically significant at every measuring point (AST1, AST2 and AST3), both nasally and temporally. No significant interactions were found between the variables group (Marfan or control) and area (nasal or temporal) (three-way ANOVA, $F(1, 167)=3.40$, $p=0.07$, $\eta_p^2=0.01$), or between the variables group and distance from the spur (three-way ANOVA, $F(2, 222)=0.13$, $p=0.87$, $\eta_p^2=0.001$).

No significant correlations were detected between AST and axial length, neither in the overall study group, nor in the MFS and control groups. For AST and spherical equivalent, only one statistically significant correlation was observed. In the MFS group, a positive correlation was observed between the spherical equivalent and AST1 on the temporal side (Pearson $r=0.402$, $p=0.047$). Patients with ectopia lentis (n=18) exhibited lower AST values compared to those without ectopia lentis (n=10) (Figure 2). This difference was statistically significant for AST3 on the temporal side (independent *t*-test, $p=0.023$). In patients with MFS, a positive correlation was observed between central corneal thickness (CCT) (Pentacam HR values) and AST for AST2, AST3, and mean AST on the nasal side (Spearman $r=0.437$, $p=0.020$; $r=0.399$, $p=0.036$; $r=0.427$, $p=0.023$; respectively for AST2, AST3 and mean AST) and for AST3 on the temporal side (Spearman $r=0.417$, $p=0.030$). In contrast, no correlation between AST and CCT was found in the control group.

In patients with a (likely) pathogenic variant associated with haploinsufficiency, AST tended to be lower compared to patients with a variant associated with a dominant negative effect (independent *t*-test; $p=0.069$, $p=0.162$, $p=0.235$, $p=0.036$ for mean AST, AST1, 2 and 3 temporally and $p=0.025$, $p=0.071$, $p=0.023$, $p=0.038$ for mean AST, AST1, 2 and 3 nasally respectively). Patients with a splice-site (n=1) and missense variant with cysteine loss (n=1) were excluded from further subgroup analysis. On the nasal side, patients with a frameshift variant had significantly lower AST compared to patients with a missense variant resulting in cysteine loss ($p=0.010$ for AST1, $p=0.026$ for AST2 and $p=0.031$ for AST3 nasally). Findings on the temporal side were non-significant. The relationship between scleral thickness and the type of (likely) pathogenic variant is depicted in Figure 3.

DISCUSSION

In this case-control study, quantitative OCT-based analysis was performed to objectively assess the anterior scleral thickness in patients with MFS. At all measuring points, temporally and nasally, the anterior sclera was significantly thinner in patients with MFS compared to matched controls. Corneal features, including thinning and flattening of the central and peripheral cornea, in patients with MFS have been well-documented in previous studies (Konradsen et al. 2012; Drolsum et al. 2015; Kinori et al. 2017). Findings of this study confirm that MFS-related thinning of the outer collagenous coat of the eye is not limited to the transparent cornea but occurs in the anterior sclera as well. Of note, anterior scleral thickness also correlated with central corneal thickness in patients with MFS in this study, particularly at the 2- and 3-mm mark. These findings add to a growing knowledge of the scleral and ciliary body characteristics in patients affected by MFS. A prior study of our group demonstrated that the anterior scleral curvature was significantly flatter in patients with MFS as compared to matched controls (Vanhonsebrouck et al. 2021). A recent study from Jia and associates also documented a significant thinning of the ciliary body in patients with MFS with the use of ultrasound biomicroscopy (Jia et al. 2023). In the past, corneal thinning in MFS has been attributed to global eye enlargement – resulting in overall thinning of the outer collagenous coat – or structural disorganisation within the tissue due to shortage of normal fibrillin-1 (Sultan et al. 2002). Both in this study, and in the beforementioned study by Jia et al., no correlation between scleral and ciliary body thinning respectively and axial length was found (Jia et al. 2023). The observed alterations in scleral architecture might stem from intrinsic disorganisation within the scleral tissue itself, be the result of eye elongation, or represent an interplay of both. Within connective tissue, fibrillin-1 deficiency results in dysregulation of TGF-beta signaling, which in turn induces high expression of matrix metalloproteinases and causes proteolytic microfibril degradation of connective tissues, such as the sclera (Wheatley et al. 1995; Neptune et al. 2003).

Similar to the observed association between ciliary body biometry and ectopia lentis (Jia et al. 2023), this study also revealed reduced scleral thickness values among patients with MFS-associated ectopia lentis. Reduced anterior scleral and ciliary body thickness, in addition to a flatter scleral curvature, suggests that zonular fibres need to bridge a larger distance from the ciliary epithelium up to the lens equator in MFS eye (Vanhonsebrouck et al. 2021)). Jia and associates additionally found the most likely direction of lens (sub)luxation to occur in the opposite direction of the thinnest area of the ciliary body (Jia et al. 2023). One could hypothesise that ectopia lentis is more likely to occur opposite to the area of anterior scleral and ciliary thinning, particularly if that region additionally has a flatter curvature. In this study, anterior scleral thickness in the vertical and oblique meridians was not assessed, neither was the sulcus-to-sulcus distance, yet it would be of value to include these items in future research, particularly in relation to ectopia lentis.

As in previous reports, the majority of (likely) pathogenic *FBN1* variants in this study were missense variants (61%), whereas 39% were predicted to exhibit a haploinsufficient effect (Robinson et al. 2002; Milewicz et al. 2021). Haploinsufficiency-associated variants resulted in lower AST values than variants

considered to have a dominant negative effect, both nasally and temporally. This finding suggests a genotype-phenotype association, with variants causing quantitative effects, potentially via its effect on TGF-beta signalling, leading to lower scleral thickness compared to those causing qualitative effects. No significant differences in AST were found when comparing specific subdivisions of (likely) pathogenic variants, except for a significantly lower nasal AST in patients with MFS with frameshift variants compared to those with missense variants resulting in cysteine loss. However, due to the limited number of patients in each category, these findings should be interpreted cautiously.

In both controls and MFS, the anterior sclera was thinner temporally than nasally, which is in agreement with prior research by Fernandez-Vigo and associates, who assessed AST using swept-source OCT in a healthy study population (Fernandez-Vigo et al. 2022). Scleral thickness exhibited an increase in thickness with distance from the scleral spur in both groups, with a significantly thicker sclera at 3 mm from the limbus compared to 1mm and 2mm. Additionally, lower temporal scleral thickness measurements were detected in patients with ectopia lentis as compared to MFS patients without lens (sub)luxation. As MFS-associated ectopia lentis often requires corrective surgery, these biometric characteristics should be taken into account (Fuchs 1997). Scleral-fixated intraocular lenses are frequently used to provide optical correction in these cases and are typically positioned 2 mm posterior to the limbus (Jacob et al. 2020). As the anterior sclera is significantly thicker at the 3 mm point in patients with MFS, placement of sutured scleral-fixated intraocular lenses at the 3 mm position may improve stability and safety of these lenses in patients with MFS.

This study had several limitations. Findings of this single-centre study should be validated by a multicentre study with larger sample sizes. In this study, full-thickness measurements were analysed in both healthy controls and patients with MFS. Future research would ideally include delineation of episcleral and scleral tissue, to assess MFS-related changes in further detail. At the execution of this study, there was no consensus in literature on how to reliable delineate the different layers using SD-OCT. Recent research of Teeuw et al. does indicate promising results to allow this in the future. Only the horizontal plane (nasal and temporal) was assessed in this study. To further investigate the link between lens subluxation, scleral and ciliary body thickness, analysis of both the anterior sclera in four axes, particularly the oblique axis, would be of particular interest. Patients with MFS who had a history of scleral surgery were excluded, which may have excluded the more severe phenotypes requiring such surgeries. Including these patients in future studies would be interesting, although the potential influence of sclerotomies on scleral thickness should be considered. As a secondary analysis, correlations between scleral thickness and clinicogenetical characteristics was conducted. The limited sample size precluded a more extensive analysis. Given the findings of significant changes in AST between Marfan patients and controls, future studies including additional inter-group analyses with larger sample sizes would be of particular benefit.

In conclusion, anterior segment OCT measurements revealed a significant reduction in AST among patients with MFS compared to age-, gender-, and axial length-matched controls. Additionally, patients with MFS and ectopia lentis and specific genetic variants exhibited lower AST values. These findings expand the current knowledge of ocular characteristics in patients with MFS.

ACKNOWLEDGEMENTS

No funding support. All authors state to have no conflict of interest regarding the study.

REFERENCES

Boote C, IA Sigal, R Grytz, Y Hua, TD Nguyen & MJA Girard (2020): Scleral structure and biomechanics. Prog Retin Eye Res **74**: 100773.

Deramo VA, CL Haupert, S Fekrat & EA Postel (2001): Hypotony caused by scleral buckle erosion in Marfan syndrome. American journal of ophthalmology **132**: 429-431.

Drolsum L, S Rand-Hendriksen, B Paus, OR Geiran & SO Semb (2015): Ocular findings in 87 adults with Ghent-1 verified Marfan syndrome. Acta Ophthalmol **93**: 46-53.

Fernandez-Vigo JI, H Shi, B Burgos-Blasco, S Fernandez-Aragon, L De-Pablo-Gomez-de-Liano, B Kudsieh, A Macarro-Merino & J Angel Fernandez-Vigo (2022): Anterior scleral thickness dimensions by swept-source optical coherence tomography. Clinical & experimental optometry **105**: 13-19.

Fuchs J (1997): Marfan syndrome and other systemic disorders with congenital ectopia lentis. A Danish national survey. Acta Paediatr **86**: 947-952.

Holbrook JA, G Neu-Yilik, MW Hentze & AE Kulozik (2004): Nonsense-mediated decay approaches the clinic. Nature genetics **36**: 801-808.

Jacob S, DA Kumar & NK Rao (2020): Scleral fixation of intraocular lenses. Curr Opin Ophthalmol **31**: 50-60.

Jia WN, QY Wang, LL Niu, ZX Chen & YX Jiang (2023): Morphometric Assessment of the Ciliary Body in Patients With Marfan Syndrome and Ectopia Lentis: A Quantitative Study Using Ultrasound Biomicroscopy. Am J Ophthalmol **251**: 24-31.

Kinori M, S Wehrli, IS Kassem, NF Azar, IH Maumenee & MB Mets (2017): Biometry Characteristics in Adults and Children With Marfan Syndrome: From the Marfan Eye Consortium of Chicago. Am J Ophthalmol **177**: 144-149.

Kommula H, SI Murthy, A Loomba, A Mohamed & R Ranjan (2023): Scleral thickness in normal Indian eyes measured using spectral domain anterior segment optical coherence tomography. Indian J Ophthalmol **71**: 1833-1836.

Konradsen TR, A Koivula, M Kugelberg & C Zetterström (2012): Corneal curvature, pachymetry, and endothelial cell density in Marfan syndrome. Acta Ophthalmol **90**: 375-379.

Linde L & B Kerem (2008): Introducing sense into nonsense in treatments of human genetic diseases. Trends Genet **24**: 552-563.

Loeys BL, HC Dietz, AC Braverman, BL Callewaert, J De Backer, RB Devereux, Y Hilhorst-Hofstee, G Jondeau, L Faivre, DM Milewicz, RE Pyeritz, PD Sponseller, P Wordsworth & AM De Paepe (2010): The revised Ghent nosology for the Marfan syndrome. Journal of medical genetics **47**: 476-485.

Milewicz DM, AC Braverman, J De Backer, SA Morris, C Boileau, IH Maumenee, G Jondeau, A Evangelista & RE Pyeritz (2021): Marfan syndrome. Nature reviews. Disease primers **7**: 64.

Muiño-Mosquera L, H De Wilde, D Devos, D Babin, L Jordaens, A Demolder, K De Groote, D De Wolf & J De Backer (2020): Myocardial disease and ventricular arrhythmia in Marfan syndrome: a prospective study. Orphanet J Rare Dis **15**: 300.

Muiño-Mosquera L, F Steijns, T Audenaert, I Meerschaut, A De Paepe, W Steyaert, S Symoens, P Coucke, B Callewaert, M Renard & J De Backer (2018): Tailoring the American College of Medical Genetics and Genomics and the Association for Molecular Pathology Guidelines for the Interpretation of Sequenced Variants in the FBN1 Gene for Marfan Syndrome: Proposal for a Disease- and Gene-Specific Guideline. Circ Genom Precis Med **11**: e002039.

Nemet AY, EI Assia, DJ Apple & IS Barequet (2006): Current concepts of ocular manifestations in Marfan syndrome. Survey of ophthalmology **51**: 561-575.

Neptune ER, PA Frischmeyer, DE Arking, L Myers, TE Bunton, B Gayraud, F Ramirez, LY Sakai & HC Dietz (2003): Dysregulation of TGF-beta activation contributes to pathogenesis in Marfan syndrome. Nat Genet **33**: 407-411.

Oyewole KT, AJ Shortt, Y Ramkissoon & PM Sullivan (2011): Simultaneous extrusion and intrusion of a scleral buckle in a patient with Marfan's syndrome. BMJ Case Rep **2011**: 2182.

Popp MW & LE Maquat (2016): Leveraging Rules of Nonsense-Mediated mRNA Decay for Genome Engineering and Personalized Medicine. Cell **165**: 1319-1322.

Robinson PN, P Booms, S Katzke, M Ladewig, L Neumann, M Palz, R Pregla, F Tiecke & T Rosenberg (2002): Mutations of FBN1 and genotype-phenotype correlations in Marfan syndrome and related fibrillinopathies. Hum Mutat **20**: 153-161.

Rodríguez-Ares MT, R Touriño, C Capeans & M Sánchez-Salorio (1999): Repair of scleral perforation with preserved scleral and amniotic membrane in Marfan's syndrome. Ophthalmic Surg Lasers **30**: 485-487.
Sharifipour FMD, MMD Panahi-Bazaz, MMD Malekahmadi & AMD Takhtaeian (2013): Spontaneous Scleral Perforation and Optic Nerve Dural Ectasia in Marfan Syndrome. Iranian Journal of Ophthalmology **25**: 167-170.
Stanciu PE, A O'Regan & E Cosgrave (2022): Late onset sclerotomy dehiscence in a patient with Marfan syndrome presenting as recurrent episodes of raised intraocular pressure. BMJ Case Rep **15**.
Sultan G, C Baudouin, O Auzerie, M De Saint Jean, M Goldschild & PJ Pisella (2002): Cornea in Marfan disease: Orbscan and in vivo confocal microscopy analysis. Invest Ophthalmol Vis Sci **43**: 1757-1764.
Teeuw GJ, DPC Vergouwen, WD Ramdas, L Sanchez-Brea, D Andrade De Jesus, A Rothova, JR Vingerling & JC Ten Berge (2023): Assessment of conjunctival, episcleral and scleral thickness in healthy individuals using anterior segment optical coherence tomography. Acta ophthalmologica.
Turaga K, S Senthil & S Jalali (2016): Recurrent spontaneous scleral rupture in Marfan's syndrome. BMJ Case Rep **2016**.
Vanhonsebrouck E, A Consejo, PJ Coucke, BP Leroy & EO Kreps (2021): The corneoscleral shape in Marfan syndrome. Acta ophthalmologica **99**: 405-410.
Voulgari N, C Giacuzzo, A Schalenbourg & GD Kymionis (2019): Occult Spontaneous Ocular Perforation Presenting as Conjunctival Chemosis in a Patient with Marfan's Syndrome. Case Rep Ophthalmol **10**: 344-348.
Wheatley HM, EI Traboulsi, BE Flowers, IH Maumenee, D Azar, RE Pyeritz & JA Whittum-Hudson (1995): Immunohistochemical localization of fibrillin in human ocular tissues. Relevance to the Marfan syndrome. Arch Ophthalmol **113**: 103-109.
Wojtkowski M, T Bajraszewski, I Gorczyńska, P Targowski, A Kowalczyk, W Wasilewski & C Radzewicz (2004): Ophthalmic imaging by spectral optical coherence tomography. American journal of ophthalmology **138**: 412-419.

FIGURES

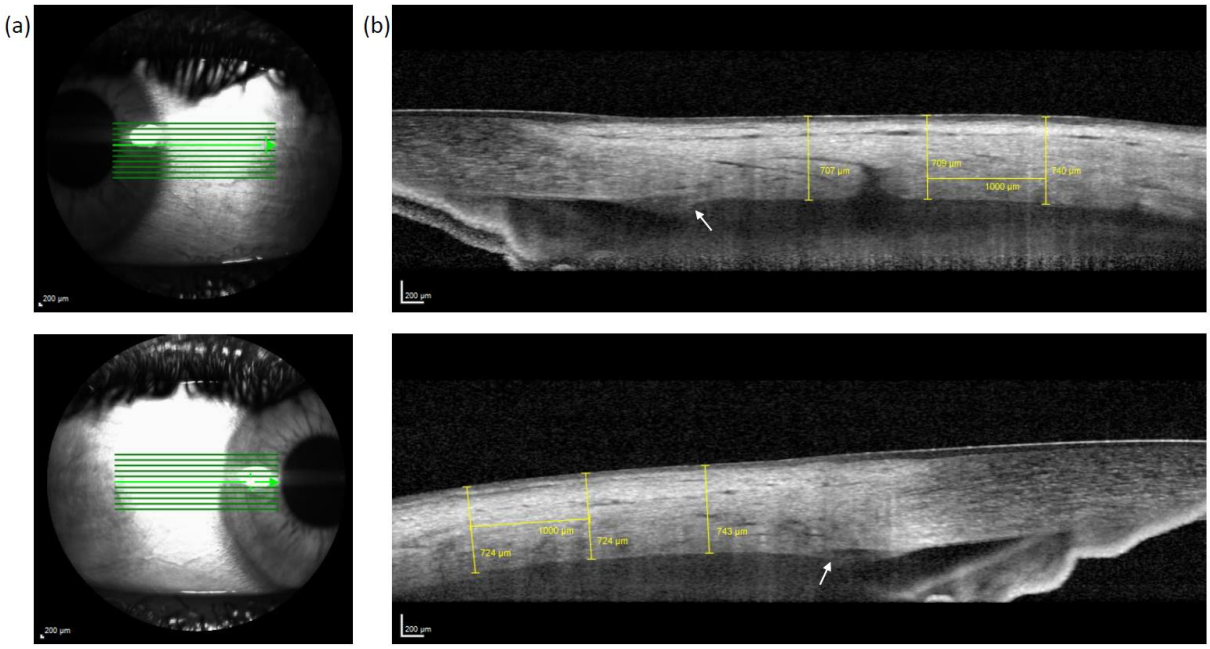

Figure 1. Anterior segment OCT scans, which demonstrates the acquisition (a) and measurement of AST1, AST2 and AST3, shown in yellow (b). Scans were obtained from the temporal and nasal sclera, with fixation in the opposite direction. The measurement of scleral thickness included the conjunctiva and episclera as shown in the photograph. AST1, AST2 and AST3 = anterior scleral thickness at 1, 2 and 3mm from the scleral spur. The scleral spur is indicated with a white arrow.

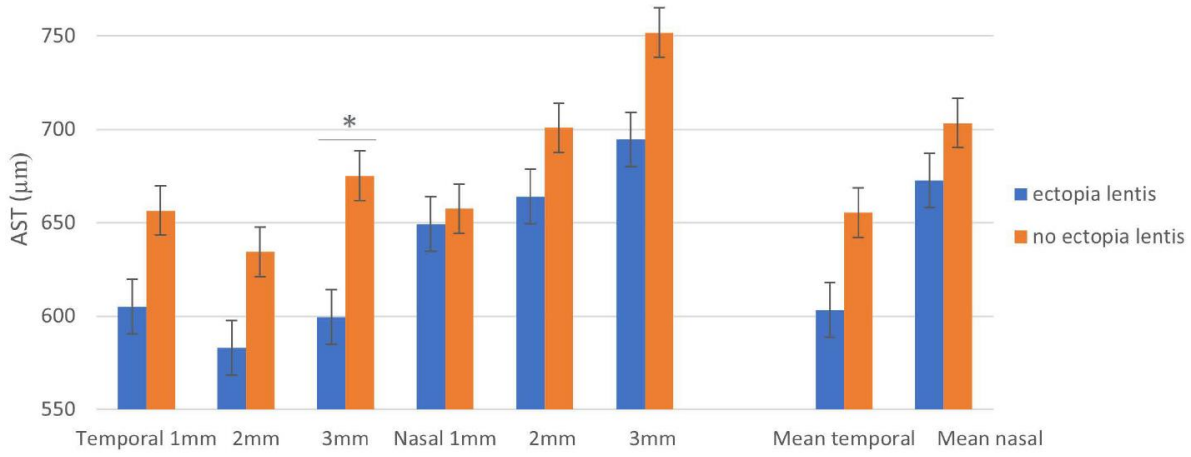

Figure 2. Mean AST (µm) on temporal and nasal side, measured 1, 2, and 3mm posterior to the scleral spur in 18 eyes of patients with MFS patients with ectopia lentis compared to 10 eyes of patients with MFS patients without ectopia lentis. Error bars with the standard error are shown. Significance ($p<0.05$) is represented by an asterisk.

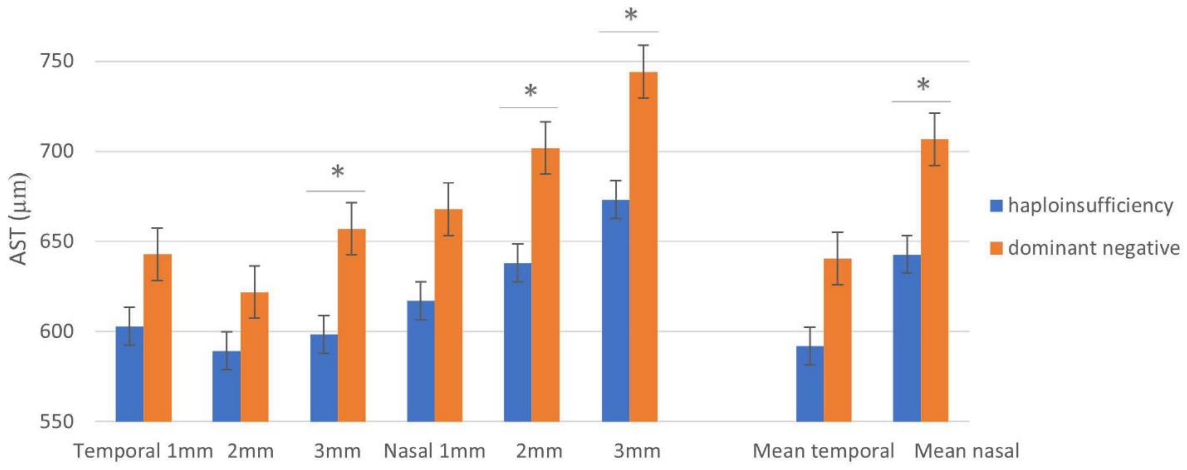

Figure 3. Mean AST (µm) on temporal and nasal side, measured 1, 2, and 3mm posterior to the scleral spur in 11 eyes of patients with MFS patients with a (likely) pathogenic variant associated with haploinsufficiency compared to 17 eyes of patients with MFS patients with a (likely) pathogenic variant considered to exhibit a dominant negative effect. Error bars with the standard error are shown. Significance ($p<0.05$) is represented by an asterisk.

TABLES

Table 1. Demographic and clinical data of patients with MFS and controls

	MFS	Controls
Number of patients	28	28
Age (y), mean ± SD	34.1 ± 12.9	31.8 ± 9.4
Eye, n right/left	25/3	26/2
Sex, n (%)		
Male	13 (46.4%)	13 (46.4%)
Female	15 (53.6%)	15 (53.6%)
Axial length (mm), mean ± SD *	24.4 ± 1.5	24.4 ± 1.3
Spherical equivalent (D), mean *	-3.36	-2.16
Central corneal thickness (CCT; µm)	526.1 ± 42.1 °	552.4 ± 30.2
Mean anterior keratometry (Kmean; D)	41.0 ± 1.6 °°	43.3 ± 1.6

y = year, SD = standard deviation, D = dioptres
* Values of the included eyes (one eye per patient) are reported.
° statistically significantly lower CCT in MFS (Mann-Whitney *U* test, p=0.003) (Pentacam HR values)
°° statistically significantly lower Kmean in MFS (independent *t*-test, p<0.001) (Pentacam HR values)

Table 2. Clinical and genetic data of MFS group

Feature	N (%)
Ectopia lentis	
Absent	10 (35.7%)
Present	18 (64.3%)
Aortic root dilatation	
Absent	4 (14.3%)
Present	24 (85.7%)
Systemic score	
< 7	6 (21%)
≥ 7	15 (54%)
Data unavailable	7 (25%)
***FBN1* variants**	
Haploinsufficiency	11 (39%)
Nonsense *	2 (7%)
Frameshift *	8 (29%)
Splice-site	1 (4%)
Dominant negative effect	17 (61%)
Nonsense **	0 (0%)
Frameshift **	0 (0%)
In-frame	0 (0%)
Missense	17 (61%)
Cysteine loss	9 (32%)
Cysteine addition	1 (4%)
No cysteine changes	7 (25%)

* nonsense and frameshift variants with no effect on exon 65 or the last 50 nucleotides of exon 64
** nonsense and frameshift variants with an effect on exon 65 or the last 50 nucleotides of exon 64

Table 3. Anterior scleral thickness (AST) in MFS and control group

Area	Distance from spur	AST (µm) MFS	AST (µm) Control	p-values
Nasal	**1mm**	648 ± 73	712 ± 69	<0.001
	2mm	677 ± 74	742 ± 67	<0.001
	3mm	716 ± 89	772 ± 78	0.008
	Total	680 ± 83	742 ± 75	<0.001
Temporal	**1mm**	627 ± 73	724 ± 88	<0.001
	2mm	609 ± 70	704 ± 82	<0.001
	3mm	635 ± 71	722 ± 80	<0.001
	Total	624 ± 71	716 ± 83	<0.001
Total	**1mm**	638 ± 73	718 ± 79	<0.001
	2mm	643 ± 79	723 ± 77	<0.001
	3mm	677 ± 90	747 ± 82	<0.001
	Total	652 ± 82	729 ± 80	<0.001

Mean values ± standard deviation of AST in different areas of analysis (nasal/temporal) and distance from the scleral spur are listed. P-values were calculated using independent Student's t-tests.